



Deposited via The University of Sheffield.

White Rose Research Online URL for this paper:

<https://eprints.whiterose.ac.uk/id/eprint/853/>

Article:

Wang, J.B., Wang, W.Y., Jewell, G.W. et al. (1998) A novel spherical permanent magnet actuator with three degrees-of-freedom. *IEEE Transactions on Magnetics*, 34 (4 (Par)). pp. 2078-2080. ISSN: 0018-9464

<https://doi.org/10.1109/20.706803>

Reuse

Items deposited in White Rose Research Online are protected by copyright, with all rights reserved unless indicated otherwise. They may be downloaded and/or printed for private study, or other acts as permitted by national copyright laws. The publisher or other rights holders may allow further reproduction and re-use of the full text version. This is indicated by the licence information on the White Rose Research Online record for the item.

Takedown

If you consider content in White Rose Research Online to be in breach of UK law, please notify us by emailing eprints@whiterose.ac.uk including the URL of the record and the reason for the withdrawal request.

A Novel Spherical Permanent Magnet Actuator with Three Degrees-of-Freedom

Jiabin Wang, Weiya Wang, Geraint W. Jewell and David Howe

Department of Electronic and Electrical Engineering, the University of Sheffield, Mappin Street, Sheffield, S1 3JD, U.K.

Abstract — The paper describes a new version of spherical actuator, which is capable of three degrees-of-freedom and a high specific torque. The three-dimensional magnetic field distribution is established using an analytical technique formulated in spherical co-ordinates, and enables the torque vector and back-emf to be derived in closed forms. This facilitates the characterisation of the actuator, and provides the foundation for design optimisation, actuator dynamic modelling and servo control development.

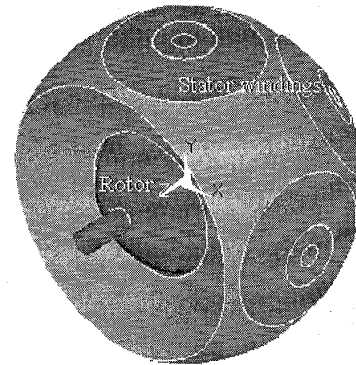
I. INTRODUCTION

There is a growing need for programmable servo-controlled high-speed actuation in multiple axes, for applications as diverse as robotic manipulators, infra-red and laser tracking systems, and automated manufacturing. At present, multi-degree-of-freedom motions are realised almost exclusively by using a separate motor/actuator for each axis, which results in relatively complicated and heavy transmission systems. This inevitably compromises the dynamic performance and servo-tracking accuracy, due to the combined effects of inertia, backlash, non-linear friction, and elastic deformation of gears. Actuators with multiple degrees-of-freedom should alleviate these problems, whilst being lighter and more efficient. However, although they have been the subject of research for several decades, and numerous concepts have been proposed [1]-[4], their application potential has not been realised, probably due to the complexity of their structure and related difficulties in modelling their electromagnetic behaviour and optimising their design.

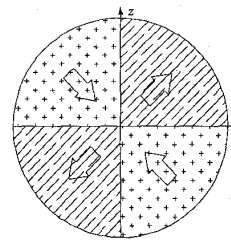
Recently, a new form of spherical actuator, which is capable of two degrees-of-freedom, has been described, systematically analysed and experimentally demonstrated [5], [6]. This paper describes a more advanced version, shown schematically in Fig.1(a), which is capable of *three degrees-of-freedom*. The actuator has a four-pole spherical permanent magnet rotor, which is formed from two pairs of parallel magnetised quarter-spheres, as shown in Fig. 1(b), and a simple stator winding arrangement. The spherical rare-earth magnet rotor is housed within the spherical stator on a low friction surface coating. Accommodated on the stator are four sets of windings, as shown Fig. 1(c), which are arranged so that three independently controllable torque components can be developed by energising the appropriate windings. The stator can be either air-cored or iron-cored by enclosing the windings with a spherical iron shell so as to increase the torque capability.

II. MAGNETIC FIELD DISTRIBUTION

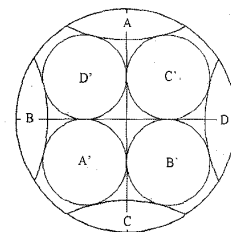
A knowledge of the magnetic field distribution produced



(a)



(b)



(c)

Fig. 1 Schematic of a 3 DOF spherical actuator. (a) Schematic. (b) rotor magnetisation pattern. (c) winding arrangement (rear view).

by the spherical permanent magnet rotor is fundamental to establishing an accurate model of the actuator, for design optimisation and dynamic modelling. Without loss of generality, an air-cored actuator is considered. Thus, the entire magnetic field region can be divided into two sub-regions, the outer airspace/winding region in which the permeability is μ_0 , and the magnet region in which the permeability is $\mu_0\mu_r$. Therefore:

$$B = \begin{cases} \mu_0 H & \text{in the airspace/windings} \\ \mu_0\mu_r H + \mu_0 M & \text{in the magnet} \end{cases} \quad (1)$$

where μ_r is the relative recoil permeability of the magnet and M is its remanent magnetization. For a permanent magnet having a linear demagnetization characteristic, μ_r is constant and M is related to the remanence, B_{rem} , by $M = B_{rem}/\mu_0$. It is convenient to formulate the field distribution in terms of a scalar potential, φ defined as $H = -\nabla\varphi$, and the spherical co-ordinate system shown in Fig. 2. This leads to the following field equations:

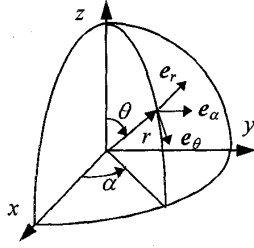


Fig. 2 Spherical Co-ordinate system

$$\begin{cases} \nabla^2 \phi_I = 0 & \text{in the airspace/windings} \\ \nabla^2 \phi_{II} = \nabla \cdot \mathbf{M} / \mu_r & \text{in the magnet} \end{cases} \quad (2)$$

The components of the magnetisation vector \mathbf{M} shown in Fig. 1(b) may be expressed as:

$$\begin{cases} M_r = M_c [\text{sgn}(\tan \theta) \sin \theta \sin \alpha + \text{sgn}(\sin \alpha) \cos \theta] \\ M_\theta = M_c [\text{sgn}(\tan \theta) \cos \theta \sin \alpha - \text{sgn}(\sin \alpha) \sin \theta] \\ M_\alpha = M_c [\text{sgn}(\tan \theta) \cos \alpha] \end{cases} \quad (3)$$

where $\text{sgn}(\cdot)$ denotes the sign function and $M_c = B_{rem} / \mu_0 \sqrt{2}$. It can be shown that $\nabla \cdot \mathbf{M} = 0$. However, the contribution of the magnets will appear in the following interface boundary conditions:

$$\begin{cases} -\mu_r \left. \frac{\partial \phi_{II}}{\partial r} \right|_{r=R_m} + M_r = -\left. \frac{\partial \phi_I}{\partial r} \right|_{r=R_m} \\ \left. \frac{1}{r} \frac{\partial \phi_{II}}{\partial \theta} \right|_{r=R_m} = -\left. \frac{1}{r} \frac{\partial \phi_I}{\partial \theta} \right|_{r=R_m} \\ \left. \frac{1}{r \sin \theta} \frac{\partial \phi_{II}}{\partial \alpha} \right|_{r=R_m} = -\left. \frac{1}{r \sin \theta} \frac{\partial \phi_I}{\partial \alpha} \right|_{r=R_m} \end{cases} \quad (4)$$

where R_m is the radius of the spherical rotor. The radial component, M_r , may be expanded into spherical harmonics of the following form:

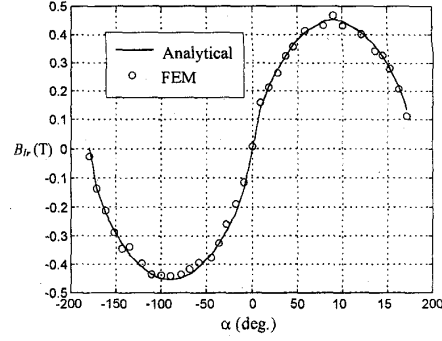
$$M_r = \sum_{l=2,4,\dots}^{\infty} \sum_{m=1,3,\dots}^l M_{lm} P_l^m(\cos \theta) \sin \alpha \quad (5)$$

where $P_l^m(\cdot)$ denotes the associated Legendre polynomial of degree l and order m , and M_{lm} is given by:

$$M_{lm} = \frac{4(2l+1)(l-m)!}{\pi m(l+m)!} M_c \int_0^1 P_l^m(x) x dx \quad (6)$$

Solving for equation (2) with the boundary conditions of equation (4) yields the following expressions for the flux density distribution in the airspace/winding region:

$$\begin{aligned} B_{I\theta} &= \sum_{l=2,4,\dots}^{\infty} \sum_{m=1,3,\dots}^l C_{lm} (l+1) r^{-(l+2)} P_l^m(\cos \theta) \sin \alpha \\ B_{I\theta} &= \sum_{l=2,4,\dots}^{\infty} \sum_{m=1,3,\dots}^l C_{lm} r^{-(l+2)} \frac{d}{d\theta} P_l^m(\cos \theta) \sin \alpha \end{aligned} \quad (7-a)$$

Fig. 3 Radial component of flux density as a function of α at $r=0.045(\text{m})$, $\theta = 60^\circ$ for $R_m = 0.040(\text{m})$

$$B_{I\alpha} = \sum_{l=2,4,\dots}^{\infty} \sum_{m=1,3,\dots}^l \frac{m C_{lm}}{\sin \theta} r^{-(l+2)} P_l^m(\cos \theta) \cos \alpha \quad (7-b)$$

where C_{lm} is given by:

$$C_{lm} = -\mu_0 R_m^{l+2} M_{lm} / [(1+l)(1+\mu_r)]$$

This result has been validated by finite element analysis, as shown in Fig. 3, the differences between the two predictions being attributable to the effect of discretization in the finite element model.

III TORQUE AND EMF PREDICTION

The torque exerted on the rotor, resulting from the interaction between the current in a stator winding and the rotor magnetic field, is given by:

$$\mathbf{T} = - \int_V \mathbf{r} \times (\mathbf{J} \times \mathbf{B}) dV \quad (8)$$

where \mathbf{J} denotes the current density vector in the winding region V . Each winding comprises a number of circular turns distributed on the spherical stator, and occupying an area bounded by $r = R_o$, $r = R_s$, and $\delta = \delta_o$, $\delta = \delta_i$, as shown in Fig. 4. Considering a single turn with infinitesimal cross-section $ds = r dr d\delta$ and an enclosing circular contour C , the total torque produced by the winding may be obtained from the following integration:

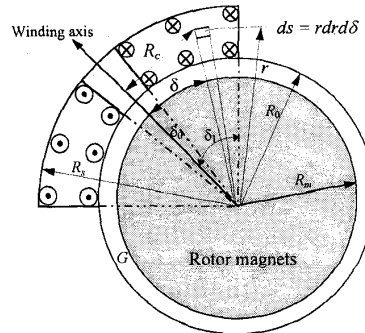


Fig. 4 Winding distribution

$$T = -2J \int_{R_0}^{R_s} \int_{\delta_0}^{\delta_1} \left\{ \int_C r B_{lr}(r, \theta) dl \right\} r dr d\delta \quad (9)$$

It can be shown that B_{lr} is dominated by its fundamental component, viz. $l = 2, m = 1$. Therefore, the result of equation (9), neglecting high order harmonics, is given by:

$$T = \begin{bmatrix} T_x \\ T_y \\ T_z \end{bmatrix} = T_m \begin{bmatrix} v_y^2 - v_z^2 \\ -v_x v_y \\ v_x v_z \end{bmatrix} \quad (10)$$

where $v = [v_x \ v_y \ v_z]^T$ is the direction cosines of the winding, viz: $v_x = \sin \theta \cos \alpha$; $v_y = \sin \theta \sin \alpha$; $v_z = \cos \theta$. The torque magnitude, T_m , is given by:

$$T_m = 15\pi\sqrt{2} B_{rem} J R_m^4 \ln(R_s / R_0) (\sin^3 \delta_1 - \sin^3 \delta_0) / (8(2\mu_r + 3)).$$

As can be seen, T_m is dependent upon B_{rem} and J as well as the geometrical parameters of the rotor and the winding. If the airgap between the rotor and winding is G , then for given B_{rem} , J , δ_0 , δ_1 and R_s , T_m is a function of R_m/R_s . This relation is plotted in Fig. 5 assuming $B_{rem} = 1.2T$, $\mu_r = 1.15$, $J = 2.0A/mm^2$, $\delta_0 = 5^\circ$, $\delta_1 = 30^\circ$, $G = 0.002m$ and $R_s = 0.042m$. It is evident that there exists an optimal ratio of R_m/R_s , viz. 0.738, that yields maximum torque.

The torque, T_c , produced by a pair of windings carrying current i and having direction cosines $[v_x \ v_y \ v_z]^T$ and $[v'_x \ v'_y \ v'_z]^T$, respectively, is given by:

$$T_c = \begin{bmatrix} T_{cx} \\ T_{cy} \\ T_{cz} \end{bmatrix} = K_T i \begin{bmatrix} v_y^2 - v_z^2 + v'_y{}^2 - v'_z{}^2 \\ -v_x v_y - v'_x v'_y \\ v_x v_z + v'_x v'_z \end{bmatrix} \quad (11)$$

where

$$K_T = T_m N / [J(R_s^2 - R_0^2)(\delta_1 - \delta_0)] \quad (12)$$

is defined as the winding torque constant, and N is the number of turns for the winding pair. The total torque, T_{em} , produced by four sets of identical windings, A, B, C, and D, having direction cosines $[v_{xj} \ v_{yj} \ v_{zj}]^T$ and $[v'_{xj} \ v'_{yj} \ v'_{zj}]^T$ ($j = A, \dots, D$) is, therefore, given by:

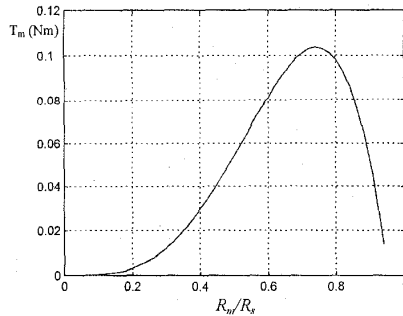


Fig. 5 Torque as a function of R_m/R_s

$$T_{em} = \sum_{j=A, \dots, D} T_{cj} = K_{TM} i \quad (13)$$

where $i = [i_A \ i_B \ i_C \ i_D]^T$ is the winding current vector, and K_{TM} , defined as the torque matrix of the actuator, is given by:

$$K_{TM} = K_T \begin{bmatrix} v_{yA}^2 - v_{zA}^2 + v_{yA}'^2 - v_{zA}'^2 & v_{yB}^2 - v_{zB}^2 + v_{yB}'^2 - v_{zB}'^2 \\ -v_{xA}v_{yA} - v_{xA}'v_{yA}' & -v_{xB}v_{yB} - v_{xB}'v_{yB}' \\ v_{xA}v_{zA} + v_{xA}'v_{zA}' & v_{xB}v_{zB} + v_{xB}'v_{zB}' \\ v_{yC}^2 - v_{zC}^2 + v_{yC}'^2 - v_{zC}'^2 & v_{yD}^2 - v_{zD}^2 + v_{yD}'^2 - v_{zD}'^2 \\ -v_{xC}v_{yC} - v_{xC}'v_{yC}' & -v_{xD}v_{yD} - v_{xD}'v_{yD}' \\ v_{xC}v_{zC} + v_{xC}'v_{zC}' & v_{xD}v_{zD} + v_{xD}'v_{zD}' \end{bmatrix} \quad (14)$$

It can be shown that the rank of K_{TM} is three within the working envelope of the actuator, implying that the actuator is able to deliver motion in three degrees-of-freedom, viz. $\pm 45^\circ$ pan-tilt excursions and continuous rotation.

By a similar integration procedure, the flux-linkage of a pair of windings due to the rotor magnetic field is given by:

$$\Psi_w = K_E (v_y v_z + v'_y v'_z) \quad (15)$$

where K_E , defined as the back-emf constant of the winding pair, is identical to K_T . The back-emfs of four identical windings A, B, C, and D are, therefore, given by:

$$e_j = -K_T \frac{d}{dt} (v_{yj} v_{zj} + v'_{yj} v'_{zj}) \quad j = A, \dots, D \quad (16)$$

IV. CONCLUSION

A new version of spherical actuator which is capable of three degrees-of-freedom has been described and analyzed. It has a four-pole spherical magnet rotor and four sets of stator windings which are arranged to produce three independent torque components. The magnetic field distribution, torque vector and back-emf have been analytically derived. The results provide a basis for design optimisation, system dynamic modelling and closed-loop control law development.

REFERENCES

- [1] K. Davey, G. Vachtsevanos and R. Powers, "The analysis of fields and torques in spherical induction motors" *IEEE Trans. on Magn.*, vol. 23, pp. 273-282, 1987.
- [2] K. Lee and C. Kwan, "Design concept development of a spherical stepper for robotic applications" *IEEE Trans. on Robot. Automat.*, vol. 7, pp. 175-181, 1991.
- [3] B. Bederson, R. Wallace and E. Schwartz, "A miniature pan-tilt actuator: the spherical pointing motor" *IEEE Trans. on Robot. Automat.*, vol. 10, pp 298-308, 1994.
- [4] K. Lee, J. Pei and R. Roth, "Kinematic analysis of a three degree of freedom spherical wrist actuator", *Mechatronics*, Vol. 4, pp581-605, 1994
- [5] J. Wang, G. W. Jewell and D. Howe, "Analysis, design and control of a novel spherical permanent magnet actuator" *IEE Proc.-Electr. Power Appl.*, in press, 1997
- [6] J. Wang, G. W. Jewell and D. Howe, "Modelling of a novel spherical permanent magnet actuator" *Proc. of IEEE Inter Conf. on Robotics and Automation*, New Mexico, U.S.A., 1190-1195, 1997.